Molecular recognition within the ES complex: A mechanistic investigation to discern how 6-hydroxynicotinate-3-monooxygenase (NicC) distinguishes between substrate analogues when enhancing its rate of NADH oxidation.

Joel K. Brown and Mark J. Snider; Department of Chemistry, The College of Wooster, Ohio

Background and Significance

- Group A flavin dependent monooxygenases catalyze the ortho or para hydroxylation of their aromatic substrates through the use of the FAD cofactor, an external electron donor (NAD(P)H) and molecular oxygen.
- The canonical reference to describe the general mechanism of the reaction of these enzymes is the mechanism of para-hydroxybenzoate hydroxylase (PHBH).
- Although PHBH is a good general reference to use when beginning to think about these enzymes, some enzymes in fact diverge from certain aspects in the mechanism of PHBH.[1,2]
- To get a more complete picture of the various mechanisms utilized by enzymes in this class when undergoing their various reactions, more members of this class need to be studied. These studies could help improve bioremediation approaches and be useful for synthetic purposes.
- NicC, a relatively newly discovered member of the Group A FAD-dependent monooxygenases catalyzes the decarboxylative hydroxylation reaction of 6-hydroxynicotinic acid (6-HNA) to 2,5-dihydroxypyridine (2,5-DHP):

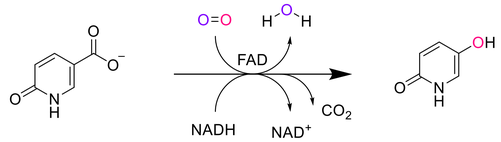

Scheme 1. Reaction catalyzed by NicC

- NicC shares two mechanistic features with PHBH: the two-step binding of their substrates involving ionization and the rate enhancement in NADH oxidation when their aromatic substrates are bound (46x increase for NicC and 17000x increase for PHBH).
- To determine if this difference in the rate enhancement in the oxidation of NADH is due to NicC having evolved a mechanism of catalysis different from PHBH, we sought to understand how the binding of 6-HNA to NicC increases the rate of NADH oxidation

Catalytic cycle of flavin-dependent monooxygenases

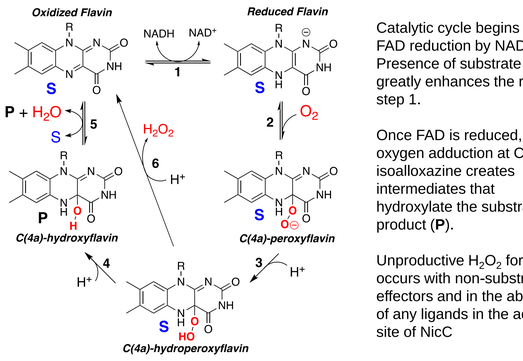

Catalytic cycle begins with FAD reduction by NADH. Presence of substrate (**S**) greatly enhances the rate of step 1.

Once FAD is reduced, oxygen adduction at C(4a) of isoalloxazine creates intermediates that hydroxylate the substrate to product (**P**).

Unproductive H_2O_2 formation occurs with non-substrate effectors and in the absence of any ligands in the active site of NicC

- Scheme 2: Role of FAD intermediates in substrate hydroxylation

Research Objectives

- Elucidate the molecular features present in 6-HNA that govern the enhanced rate of NADH oxidation in NicC
- Establish the structural determinants that NicC utilized to distinguish its substrates from non-substrate effectors

Molecular features of 6-HNA and current mechanistic proposal for decarboxylative-hydroxylation

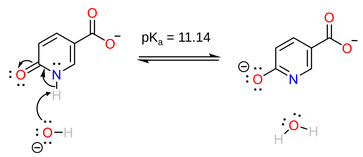

Scheme 3. Ionization by deprotonation of the pyridinolic functional group in 6-HNA

- Ionize by deprotonation
- Ion pairing via carboxylate functional group
- Hydrogen bonding via 8 hydrogen bond acceptors and one hydrogen bond donor

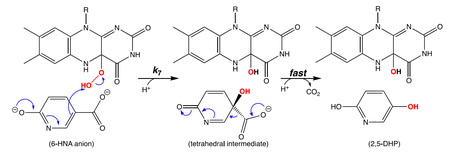

Scheme 4. Current mechanistic proposal for the hydroxylation of 6-HNA by an electrophilic aromatic substitution mechanism involving the C(4a) hydroperoxyflavin intermediate.

What molecular features in 6-HNA are used by NicC for enhancing NADH oxidation and hydroxylation?

An electronegative atom para from the carboxylate functional group is the minimum requirement for enhancing the rate of NADH oxidation in NicC

Table 1. Initial rate study of NicC saturated with various ligands ([ligand] = 10 x K_d). Plus ("+") denotes the ligands confirmed to be substrates by HPLC analysis. Rates were measured by following absorbance changes (340 – 370 nm) for NADH oxidation.

Ligand	Fraction bound	$\frac{k_{cat}^{NADH}(ligand)}{k_{cat}^{NADH}(no\ ligand)}$
No Ligand*	0	1
6-hydroxy-NA +	0.91	46.1
6-methyl-NA	< 0.56	2.3
6-chloro-NA	0.91	15.3
6-amino-NA	< 0.50	37.3
5-Cl-6-HNA +	0.91	26.4
4-HBA+	0.91	24.6
6-HN-Ald	0.91	10.0

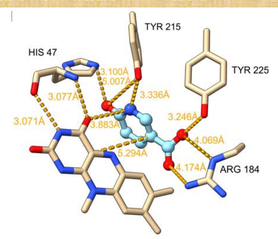

Figure 1. Predicted binding mode of 6-HNA manually modelled in active site of NicC via UCSF Chimera X. Active site residues H47, Y215 and R184 likely govern NicC's ability to recognize molecular features to enhance the rate of NADH oxidation.

Increasing capability in forming hydrogen bonds para to carboxylate functional group

Additional chlorine atom

Lack of pyridinolic nitrogen

Lack of carboxylate functional group

Ionization by deprotonation governs substrate hydroxylation

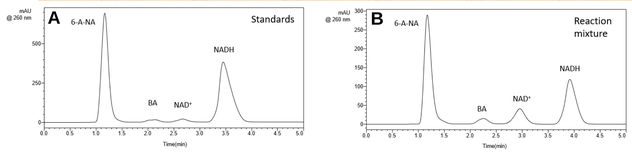

Figure 2. HPLC analysis of the reaction mixture of 6-A-NA incubated with NicC and NADH. Retention times (6-A-NA: 1.169 min, BA: 2.138, NAD+: 2.956, NADH: 3.452). (A) 200 mM NADH, 200 mM 6-A-NA, and 100 mM BA standards. No NAD+ was added but it was present in the standard, likely from the contamination of the NADH standard with NAD+. (B) Components of the reaction mixture after steady state assay. No new molecule is present in the reaction mixture, although some NADH oxidized to NAD+.

Ionization by deprotonation *may* govern the ability of the charge transfer complex to be formed and enhance the rate of NAD+ release

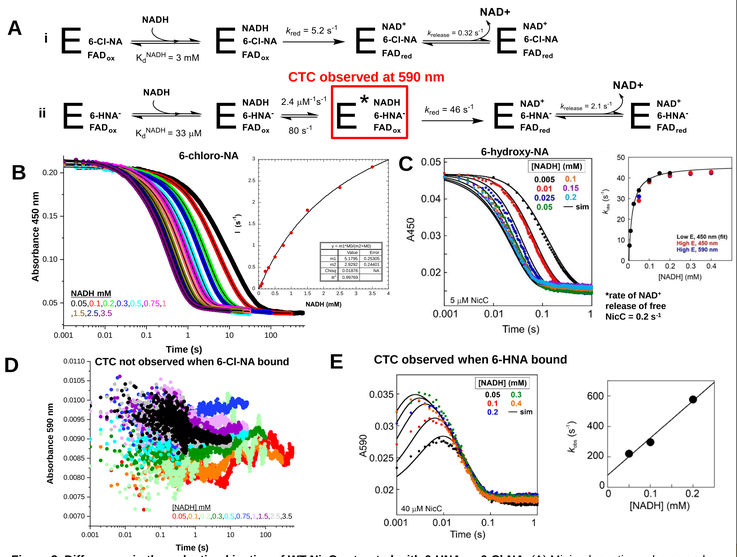

Figure 3. Differences in the reduction kinetics of WT NicC saturated with 6-HNA vs 6-Cl-NA. (A) Minimal reaction scheme and associated rate constants derived from analytical fitting to describe reduction kinetics of WT NicC saturated with (i) 6-Cl-NA and (ii) 6-HNA. (B,C) 450-nm and (D,E) 590-nm time-dependent traces from a set of reactions in which a solution of 40 μM of WT NicC and (B,D) 5mM 6-Cl-NA (10 x Kd 6-Cl-NA)[7] and (C,E) 2.5 mM 6-HNA (10 x Kd 6-HNA)[6] were mixed with an equal volume of a solution of different NADH concentrations. (Inset Plot in B and C) Plot of the eigenvalue associated with the largest amplitude obtained from (B) a triple and (C) a double exponential function against NADH concentration. (Inset Plot in E) Plot of the observed rate constants obtained from fitting the 590 reaction traces to a three-step irreversible kinetic model (*A →B →C*) against NADH concentration.

H211 and H302 are responsible for enhancing the rate of NAD+ release in WT NicC saturated with 6-HNA

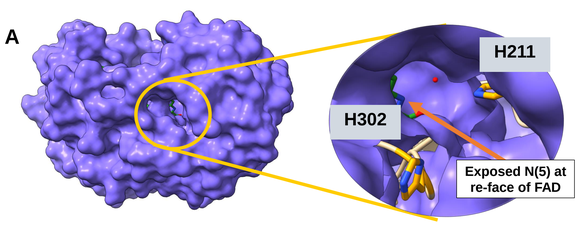

Figure 4. Reduction kinetics of the H211A and the H302A variants of NicC (A) UCSF Chimera X surface view render of a tunnel in the crystal structure of WT NicC leading to the N(5) at the re-face of FAD highlighting the residues at its entry. (B) Reduction kinetics of H211A NicC. A solution of 40 μM of WT H211A NicC saturated with 15 mM 6-HNA (10 x K_d 6-HNA for H211A NicC)[6] was rapidly mixed with an equal volume of a solution of different NADH concentrations. (C) Reduction kinetics of H302A NicC. A solution of 40 μM of WT H302A NicC saturated with 35 mM 6-HNA (10 x Kd 6-HNA for H302A NicC)[6] was rapidly mixed with an equal volume of a solution of different NADH concentrations.

Kinetic model to summarize observations:

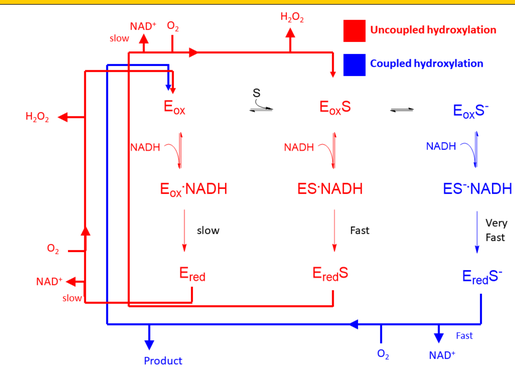

Figure 5. Simplified mechanism of NicC illustrating the three pathways NicC can use to catalyze NADH oxidation. 6-HNA can bind to NicC via a 2-step binding mechanism (shown across the top). NADH can bind with the three forms of NicC (E, $E_{ox}S$ and $E_{ox}S^-$), however the rate at which the hydride transfer occurs depends on the form of NicC. Only ligands that can be ionized by NicC (blue path) are able to be hydroxylated and yield products, whereas un-ionizable ligands result in an uncoupled reaction where NADH is oxidized but no hydroxylated product is formed. Ionization of the bound ligand also leads to an enhanced rate of NAD+ release whereas the binding of ligands that cannot ionize does not enhance the rate of NAD+ release

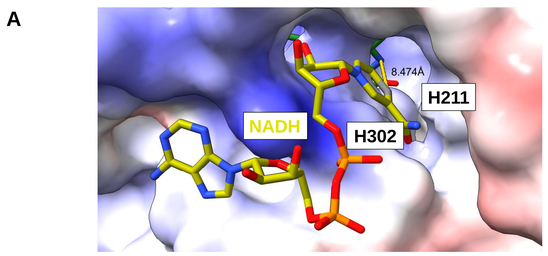

Figure 6. Proposed binding site of NADH and mechanism for NAD+ release in NicC(A) Manually modelled proposed binding mode of NADH in NicC via UCSF Chimera X[3]. (B) Simplified reaction scheme depicting the proposed ionization dependent cationic repulsion mechanism in NicC

Future Research

- Obtain high resolution crystal structures of NicC complexed with 6-HNA and Benzamide Adenine Dinucleotide in order to elucidate the mode of binding of NADH in NicC

Acknowledgements

- This work was supported by NSF Grant # 181735

References

(1) Ryan, K. S.; Chakraborty, S.; Howard-Jones, A. R.; Walsh, C. T.; Ballou, D. P.; Drennan, C. L. The FAD Cofactor of RebC Shifts to an IN Conformation upon Flavin Reduction,. Biochemistry 2008, 47 (51), 13506–13513.

(2) Hiromoto, T.; Fujiwara, S.; Hosokawa, K.; Yamaguchi, H. Crystal Structure of 3-Hydroxybenzoate Hydroxylase from Comamonas Testosteroni Has a Large Tunnel for Substrate and Oxygen Access to the Active Site. Journal of Molecular Biology 2006, 364 (5), 878–896.

(3) UCSF ChimeraX: Structure visualization for researchers, educators, and developers. Pettersen EF, Goddard TD, Huang CC, Meng EC, Couch GS, Croll TI, Morris JH, Ferrin TE. Protein Sci. 2021 Jan;30(1):70-82.

(4) Perkins, S. W.; Rajacovich, L.; Snider, M. J. Transient Kinetic Analysis of the Mechanism of 6-Hydroxynicotinate 3-Monooxygenase. Manuscript in Progress, to Be Submitted to Biochemistry.

(5) Hicks, K. A.; Yuen, M. E.; Zhen, W. F.; Gerwig, T. J.; Story, R. W.; Kopp, M. C.; Snider, M. J. Structural and Biochemical Characterization of 6-Hydroxynicotinic Acid 3-Monooxygenase, A Novel Decarboxylative Hydroxylase Involved in Aerobic Nicotinate Degradation. Biochemistry 2016, 55 (24), 3432–3446.

(6) Nakamoto, K. D.; Perkins, S. W.; Campbell, R. G.; Bauerle, M. R.; Gerwig, T. J.; Gerislioglu, S.; Wesdemiotis, C.; Anderson, M. A.; Hicks, K. A.; Snider, M. J. Mechanism of 6-Hydroxynicotinate 3-Monooxygenase, a Flavin-Dependent Decarboxylative Hydroxylase Involved in Bacterial Nicotinic Acid Degradation. 2019, 13.

(7) Campbell, R. G. A Mechanistic Investigation: Probing the Substrate Promiscuity of 6-Hydroxynicotinic Acid 3-Monooxygenase (NicC) from Bordetella Bronchiseptica RB50, Senior Independent Thesis at The College of Wooster, 2019.